Analysis and Multi-Objective Optimization of Wire Cut Process Parameters for Efficient Cutting of Tapered Carbon Steels Using Wire EDM

Muhammad Wasif*, Syed Amir Iqbal*, Yasir Ahmed Khan* and Muhammad Tufail*

**Department of Industrial and Manufacturing Engineering, NED University of Engineering and Technology, Karachi.*

Corresponding Author: wasif@neduet.edu.pk

Submitted **:** 19-10-2021

Revised **:** 24-05-2021

Accepted **:** 08-06-2021

ABSTRACT

Carbon steel AISI 2010 is a general-purpose tool steel. It is an immense need of the industry to determine the optimal process parameters for the cutting of thick slabs of metal, using the wire cut for maximum material removal rate and minimum surface roughness and wire wear. This research is designed to explore the influence of process parameters during the wire EDM of tapered steel blanks. Tapered steel blanks with angles of 30°, 45°, and 60° are machined and slots are generated in blanks using the wire EDM process. Taper angle, current, and pulse-off time are considered as the controllable process parameters for this study, whereas other controllable parameters are kept constant. Effect of these controllable parameters over kerf width, surface finish, MRR, and wire are examined using the analysis of variance technique. Regression models for the four response variables are also developed, relating the variables with the varying controllable parameters. Multi-variable optimization of controllable parameters is performed using the Genetic Algorithm for favourable response variables.

Keywords: Kerf Width; Material Removal Rate; Surface Roughness; Wire EDM, Wire Wear.

INTRODUCTION

In the class of non-traditional manufacturing processes, wire electro-discharge machining (EDM) is considered as a contemporary version of this process. It uses a conductive wire to machine metallic slabs and plates of greater thicknesses using high intensity eroding sparks (Sommer and Sommer, 2017). In machining set up, a wire acts as a cathode and metallic blank being an anode, dipped in a dielectric medium, which is cut through the eroding sparks emitting from the wire. The wire used in the process is either consumable or non-consumable, fed from a fresh spool to another wrapping spool, maintaining sufficient tension between the two spools as shown in Figure 1. The wire is fed normal to the face of the blank (inward to the cross-section plane) and controlled using the CNC controller.

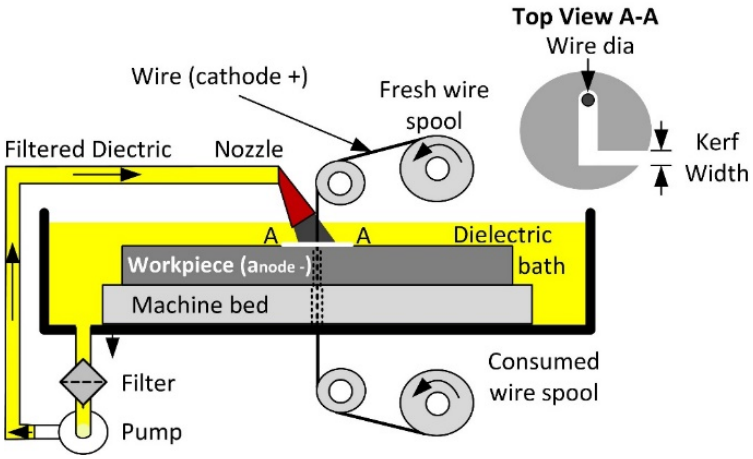

Figure 1 Components of Wire EDM process (WEDM)

Common wire materials adopted for the wire EDM process are copper, brass, and tungsten, whereas the common work piece materials are aluminium, graphite, steel, copper, tungsten, inconel, and a good range of titanium and bickel-based alloys (Sommer & Sommer, 2017; Asgar & Singholi, 2018). The latest research trends show wire experimentations with low conductive materials too, such as Polycrystalline Diamond (PCD), ceramics, and cermet (El-Hofy, 2005). Ionized water in the system serves as the standard dielectric, which provides ease in shielding the wire and blank interface and remove burrs from the erosion zone. The erosion of the blank starts with a high-frequency DC pulses, which starts a cycle of sparks and gets the material eroded in the form of particles (Sommer and Sommer 2017). The flushing pressure of the dielectric also controls the outcomes of the WEDM process, together with wire feed rate, tension, pulse on time, pulse off time, and peak current and voltage between the anode and cathodes (Jameson, 2001).

Various complicated silhouettes and contours can be produced with the help of CNC controlled wire EDM machines. Wire EDM process is widely used in manufacturing complex and intricate parts of airplanes, automotive, commercial machinery, and tool manufacturing industries due to its high productivity in terms of precision and accuracy (Jameson, 2001).

Earlier research reviews encompass the latest studies conducted on the WEDM process and can be divided into two distinct parts; one is discussing the wire EDM on other materials and second presenting the outcomes of wire EDM over the steels.

Gauri and Chakraborty (2009) applied Taguchi Method to explore the effects of pulse on time, wire feed, wire tension, peak current and delay time over the surface finish, and MRR and wire wear during the wire EDM of various materials. Majumder and Saini (2017) used Ni-Ti Alloy and titanium alloy (Ti-6Al-4V) respectively for the multi-response optimization of wire tension, wire feed, pulse rate, MRR, cutting speed, surface roughness and kerf width. Abhinesh et al. (2014) extended the research area by using titanium alloys blank and analysed the results of MRR and wire wear by changing the wire material. Kumar and Singh (2018) protracted their research study by changing the speed capacitance and electrode ratio of the wire cut for the titanium alloys. Reddy et al. (2015) diversified the analysis of kerf width by replacing titanium with aluminium alloy HE30, using the Grey Relational Analysis. Rao et al. (2016) applied the Taguchi Method to enhance the residual stress during the wire EDM of aluminium 2014 T6 alloy. Shihab (2018) optimized the pulse rate and current for a better surface finish, higher MRR, and least kerf width during the wire EDM of aluminium 5754 alloy. Shadab et al. (2019) applied optimization of pulse timing, current and wire winding rate for the highest material removal rate, and best surface finish for the metal matrix carbide. Swiercz et al. (2019) performed the finite element analysis (FEA) and experiments to build wire EDM process model to observe the influence of wire-speed, flow rate of dielectric, and tension of wire over the kerf width formed.

Due to a substantial number of steel grades and vide range of applications, several types of researches have applied different techniques to cut the steel plates through the wire EDM process. This large variety of steel has different melting points, thermal conductivity, thermal expansion, and other properties. It is entirely unproductive to apply the same WEDM process parameters over a variety of steel alloys. Hence, several researches investigated the optimal parameters and presented mathematical models for different steel grade. Huang and Liau (2003) analysed the impact of pulse rate, tension in the wire, dielectric flow rate, and wire travel

rate over the material removal rate and surface finish during the wire EDM of SKD-11 steels. Liao et al. (2004) developed analytical models for the wire EDM over the Inconel (SKD11) and discussed the effects of pulse rate over the width of the kerf, spark frequency, and surface roughness. Kanlayasiri et al. (2007) conducted his research over cold die steel (DC53) and optimized pulse-peak current, pulse-on time, pulse-off time, and wire tension for the higher surface roughness. Raksiri et al. (2010) analysed and optimized the cutting thickness error by using feed rate and the servo voltage as process parameters for the wire EDM of Inconel (SKD-11). Welling (2014) and Klocke et al. (2014) improvised the wire EDM parameters to improve the material removal rate and surface roughness for the Inconel 718. Kamei et al. (2016) observed the frequency and vibration of the wire during the wire EDM of SKD-11. They determined the effects of the wire deflection, wire tension, and position of the blank on the frequency and vibration of the wire using a high-speed camera. Takayama et al. (2016) improved the productivity of WEDM for the cutting of steel blank (SKD-11) by employing a closed-loop system, thereby improving the surface finish and wire break frequency. Babu and Soni (2017) used a similar experimental setup for the Inconel 625. Rajmohan and Kumar (2017) performed a multi-variable optimization of pulse timing, current, wire feed rate, tension in the wire and current, for the improvement in surface finish material removal rate and kerf width formed during the wire EDM of Duplex Stainless Steel (DSS). Conde et al. (2018) analysed the wire EDM outcome by varying the height of blank, dielectric pressure and pulse off duration for D2 steels blank. Sahoo et al. (2019) also optimized the main parameter for the enhancement in material removal rate, kerf width, and surface finish during the wire EDM of high-carbon and high-chromium steels. It was inferred from the results that the pulse width time is the dominant factor, while wire feed rate and pulse-off time have the least impact. Priyadarshini et al. (2019a, 2019b) adopted Grey-Taguchi Technique for the favourable kerf width and MRR during the wire EDM of P20 steel (low carbon steel) by optimizing the pulse timing and servo voltage. They performed another research on the same material by using similar process parameters and variables under a sub-cooled environment. Dayakar et al. (2019) performed multi-variable optimization of pulse rate, peak current, and servo voltage for the enhanced surface roughness and material removal rate in the wire EDM for low carbon steel (350). They also developed a regression model to relate the process parameters with MRR and surface finish. Ahmed et al. (2020) optimized the pulse-on and pulse-off time for the minimum surface roughness and maximum surface roughness, using artificial neural network (ANN). El-Bahloul (2020) conducted a similar optimization for the AISI 304 using artificial intelligence (AI) technique. Arunadevi et al. (2021) proposed another optimization-based research for the improvement in surface roughness and MRR, thus optimizing the process parameters by applying Decision Tree and Naive Bayes Algorithm.

The literature cited above discloses that several types of metal alloys have been analysed by using the wire EDM process. Steel AISI 1020 is recognized as a general-purpose low carbon steel used extensively in the automobile and aircraft industry. Machine components, such as axles, camshafts, spindles, gears, and structural parts are machined due to its excellent machinability, weldability, and hardness (BHN between 119-235). However, it has a low tensile strength range, which varies between 410-790 MPa due to low carbon contents (Dewangan et al., 2019). Due to its vast applications, it is unavoidable to study the effects of wire EDM controllable parameters over the critical process outcomes such as kerf width, surface finish, material removal rate (MRR), and wire wear. None of the above mentioned research studies focused on the outcomes of wire EDM over the varying profile workpieces. These work pieces are primarily applied in intricate automobile and aircraft parts, machine tools, and medical equipment. Due to the requirement of the industry, tapered work pieces of carbon steel alloy have been considered in this research. The influence of the taper angle has been addressed in the present research over the outcomes of wire EDM of the titanium alloy. The literature review has been keenly observed that applying the same value of process parameters for other steel grades, does not provide ideal outcomes especially the surface finish and MRR, which certainly increase the cost of the process. Industry demands to investigate the outcomes of wire EDM over the varying cross-sectional blanks of intricate shape, hence the same is considered in this research. Rather than investigating one or two outcomes, four major response variables including kerf width, surface roughness, wire wear, and MRR were analysed in this study. Unique experimental setup and post-processing techniques have been employed to analyse the effects of taper angle, current, and pulse-off time over these outcomes. A detailed discussion along with ANOVA and mean responses of the variables are also presented in the study. The regression model for all the four response variables has been developed and finally the multi-variable/multi-objective process parameter optimization has been applied for the favourable outcomes.

This article contains six sections. The first section of the research describes a thorough literature review and research problem; section two presents the experimental setup; section three includes the outcomes and analysis; section four presents the regression model; section five focuses on the multi-variable optimization of the outcomes; and the last section includes the conclusion obtained through the results.

EXPERIMENTAL SET-UP

The expected outcome of this research is to determine the optimal process parameters of wire EDM for the improved response outcomes of kerf width, surface roughness, MRR, and wire wear for the tapered blanks of AISI 1020 sheets of steel. A comprehensive research methodology having experimental design, results analysis, and other details are explained below.

Wire Cut Machine Tool

A CHMER wire cut machine tool of model CW-43F was used, having an envelope of 500mm x 350mm x 200mm along the x, y, and z-axes, respectively. Controllable wire EDM process parameters in this machine tool are a type of wire electrode, dielectric medium, serve feed (V), pulse on time (μs), pulse off-time (μs), peak current (A), feed rate of wire (mm/min), wire tension (N), and flushing pressure (psi or bar).

Tapered Blanks

A sole source for the carbon steel 1020 blank has been considered. The material properties of the steel are listed in Table 1. Tapered blanks of 30°, 45° and 60° of carbon steel 1020 are machined. A replicate of each blank is prepared to achieve accuracy for precision in analysis and to avoid biases. Hence, six blanks are prepared to cut the slots in it. The dimension of the samples is shown in Figure 2. The top view of the blank (Figure 2(a)) shows the four slots to be generated through the wire EDM on the blank. It can be seen in the front view (Figure 2(b)) of the blank that the length of the tapered face along the horizontal direction is based on the taper angle θ. Therefore, it is the longest for 30° taper angle and shortest for 60° taper angle blank. Figure 2(c) shows the taper work piece side view along with the slots to be generated.

Table 1. Material Properties of Carbon Steel 1020

Properties	Value
Chemical composition (%)	Mn(0.3), C(0.2), S(0.03), P(0.03). Fe(remaining)
Density (kg/m^3)	7870
Hardness (BHN)	111
Ultimate Tensile Strength (MPa)	380
Modulus of Elasticity (GPa)	200
Poisson's Ratio	0.29
Shear Modulus (GPa)	80
Specific Heat Capacity (J/g-°C)	0.486
Thermal Conductivity (W/m-K)	51.9
Melting Point (°C)	1500-1550

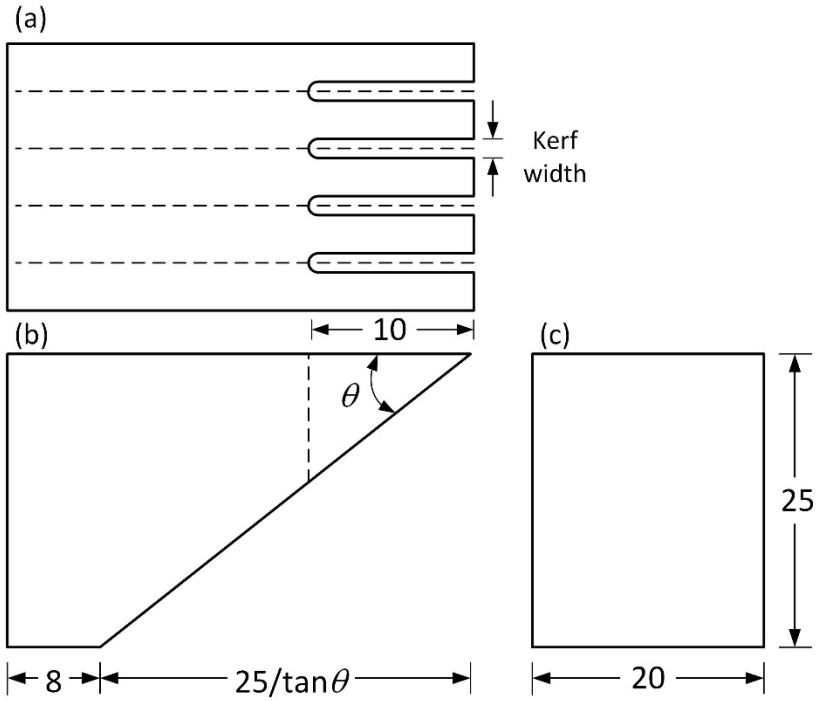

Figure 2 Tapped blank and slots cut through wire EDM, (a) top view, (b) Front view, (c) side view.

Experimental Design

In this research, a few of the most influential controllable parameters as reported in the literature review are varied, keeping others at constant values. These co8. controllable parameters, along with their levels are listed in Table 2.

Table 2. Controllable wire EDM process parameters

Parameters and Symbols	Levels		
	1	2	3
Taper Angle (A)	30°	45°	60°
Current (C)	5A	10A	--
Pulse-off time (POT)	20μs	40μs	--

The parameters or factors which are kept unchanged include brass wire material and 0.25mm diameter of it. Due to the dependency of pulse-on time and pulse-off time over each other, pulse-on time is considered constant. The constant feed rate of 3 mm/min is used with the pulse-on time of 25μs and a servo voltage of 65 volts. Wire tension is set to 12N with the wire velocity of 20 mm/min. The dielectric medium is ionized water and the flushing pressure rate is fixed at 2 litres/hour.

With a combination of parameters at all levels, twelve slots were to be generated, which were intended to be replicated twice. A total of thirty-six slots were generated using a combination of controllable parameters. Hence, on nine blanks of carbon steel, four slots were generated on each, using the wire EDM. The sequence of these experiments was kept random to drop the biasness of results. By varying the pulse off time and current setting, four cuts were made on each blank using wire EDM, along the dash lines as shown in Figure 2(a).

Response Variables

Response variables of the experiments are the outcomes of the research, which are measured on the blank or wire used in the experiments using the following modus.

Kerf width is the width of the slot produced during the erosion process (refer to Figure 1). Its enlarged images are taken through the digital microscope and are measured using the post-processing software at four various locations along the length of the slot. Tapered blanks of carbon steel 1020 are examined on the MM 500-T MTI corporation microscope with digital camera DCM 310 attached to it. Images from the top view (refer to Figure 2(a) are captured and shown in Figure 3. These images are processed through the Scope Photo 3.0 software to measure the kerf width along the slots. Along the 10 mm length of each slot, kerf widths are measured at four distinct locations of 3mm, 5mm, 7mm, and 10mm from the flat face. For each location, kerf widths are measured twice, which means kerf widths are determined to be the final kerf width. Enlarged images of kerf width are generated through the wire EDM on the six blanks. One of them is shown in Figure 3.

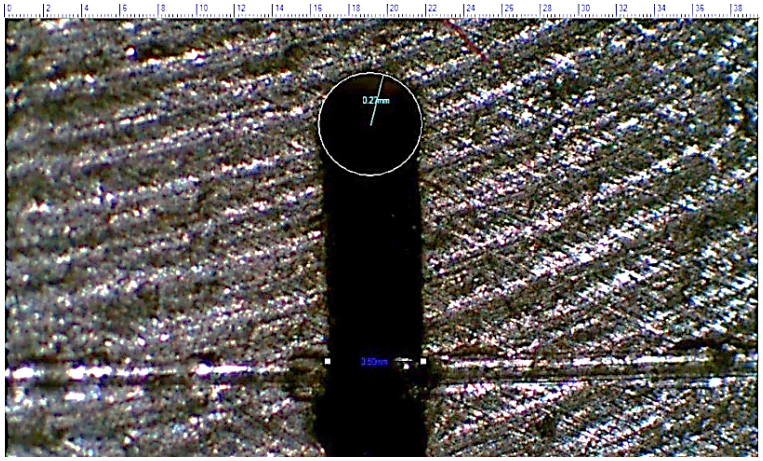

Figure 3 Kerf width of slot generated in blank with 45° taper angle (cut with Current 10A and POT 40µs)

The efficiency of the wire EDM process can be determined using the material removal rate (MRR), which is the ratio of the volume of metal removed to the machining time (Jameson 2001). Hence MRR can be determined by the following relation.

$$MRR = \frac{M_2 - M_1}{\rho \cdot t_{cut}} \quad (1)$$

Where, M_2 and M_1 are the masses of the blank before and after the cutting process, ρ is the density and t_{cut} is the time spent on cutting the slot.

The cost of wire consumed is an essential aspect of the wire EDM process, since it affects the cost of the process. Higher the velocity of wire spooling and feed, the more wire is consumed, which depends upon the type of the material being cut. Wire wear measures the percentage of wire consumed during the wire EDM process. Masses of blanks and wire are measured using a digital balance of high precision up to six digits lest the count is in a confined environment.

Surface integrity is a crucial factor in the wire EDM process and it can be achieved by measuring the surface roughness exposed to erosion. James (2001) opines that an optimal waviness curve provides a better surface finish. To measure the roughness after cutting the carbon steel blanks, they are cut using a thin rotating saw from the centre of the slots (dash lines), as shown in Figure 2(a) without damaging the eroded surfaces. Using Meiji EMZ-8TR-PBH Zoom Stereo Microscope with a magnification range of 10 to 45X, images of eroded and surfaces are captured. Contouro Matic T2 surface roughness high precision gauge with measuring capacity of up to 0.033μm is used for measuring surface roughness at three different heights of eroded surfaces. Both continuous and mean readings are taken by moving stylus of the digital gauge at the heights of 30%, 60% and 90% of steel blanks, as shown in Figure 4.

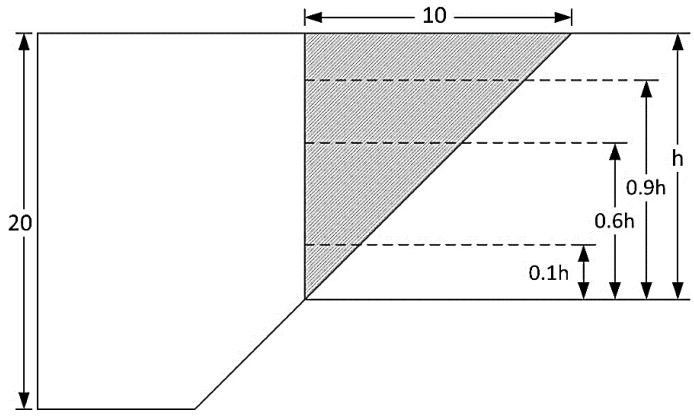

Figure 4 Cross-sectional view of the tapered work piece along the slot generated through WEDM.

Table 3 presents the mean response variables determined with the combination of process parameters in order of running experiments.

Table 3. Mean response variables determined for the set of process parameters.

Taper Angle (Degree)	Current (Ampere)	Pulse off Time (μs)	Kerf Width (mm)	Surface Roughness (μs)	MRR (mm^3/min)	Wire Wear (Percentage)
30	5	20	0.4350	0.0133	11.85	0.1592
30	5	40	0.4388	0.0098	4.72	0.1936
30	10	20	0.4825	0.0150	13.45	0.1581
30	10	40	0.4950	0.0110	9.21	0.2169
45	5	20	0.2961	0.0163	6.27	0.3501
45	5	40	0.4088	0.0218	4.20	0.7867
45	10	20	0.3638	0.0193	11.97	0.3571
45	10	40	0.3536	0.0140	8.61	0.3978
60	5	20	0.2888	0.0120	5.03	0.5331
60	5	40	0.2913	0.0170	3.32	0.8866
60	10	20	0.3588	0.0175	8.40	0.3779
60	10	40	0.3613	0.0160	6.81	0.5523

ANALYSIS

The main hypothesis (H_o) of the research suggests that the mean response variable determined with different combination of controllable parameter are equal, which indicates that no impact of controllable parameter exists over the response variable. The alternate hypothesis (H_1) suggests that the means of response variables differ for the varied controllable parameters or interactions. The hypotheses are tested over the 95% confidence interval, with the bounds of the controllable parameters as defined in Table 2. This suggests that the factor or interaction has considerable influence over the response variable. Using the wire EDM, four slots are generated in each tapered blank of carbon steel 1020 and the outcome through the response variables is evaluated as described in the methodology section. The data of controllable parameters and measured response variables are processed through the Minitab, a statistical analysis software. Each of the four-response variables is analysed and the results are discussed below.

Kerf Width

Average kerf widths along the slots at various locations and generated through different combinations of parameters are shown in Figure 5. This figure shows that the largest kerf widths are generated in the blanks having the taper angles of 30°. Larger curve widths are formed due to the high rate of erosion on the exposed surfaces. This is caused due to the least surface area of the steel blank, exposed to the spark emitting wire. In comparison, small kerf widths are observed in the tapered blanks having angles of 45° and 60°, while not following the same trends. In both types of blanks, kerf width magnitude is majorly affected by the applied current. Higher kerf widths are observed in the blanks cut with 10A, whereas smaller kerf widths are seen cut with the 5A current. Although the kerf width remains stable during the wire EDM of steel blanks, in few cases an increase in kerf width can be seen at the higher distance from the flat face. This is due to the low visible surface area exposed to the spark emitting wire.

Table 4 presents the analysis of variance (ANOVA) for the kerf width generated during the wire EDM of carbon steel 1020 by varying the process parameters. According to the P-value, less than 0.05 taper angle and current have substantial influence over the kerf width. Hence alternate hypothesis (H_1) is valid for only these two process parameters. The taper angle has the largest effect of having F-value equal to 52.94, whereas current also affects the curve width having an F-value equal to 13.83. Other parameters and their interactions do not significantly impact the kerf width, which is evident from the P-values higher than the 5%.

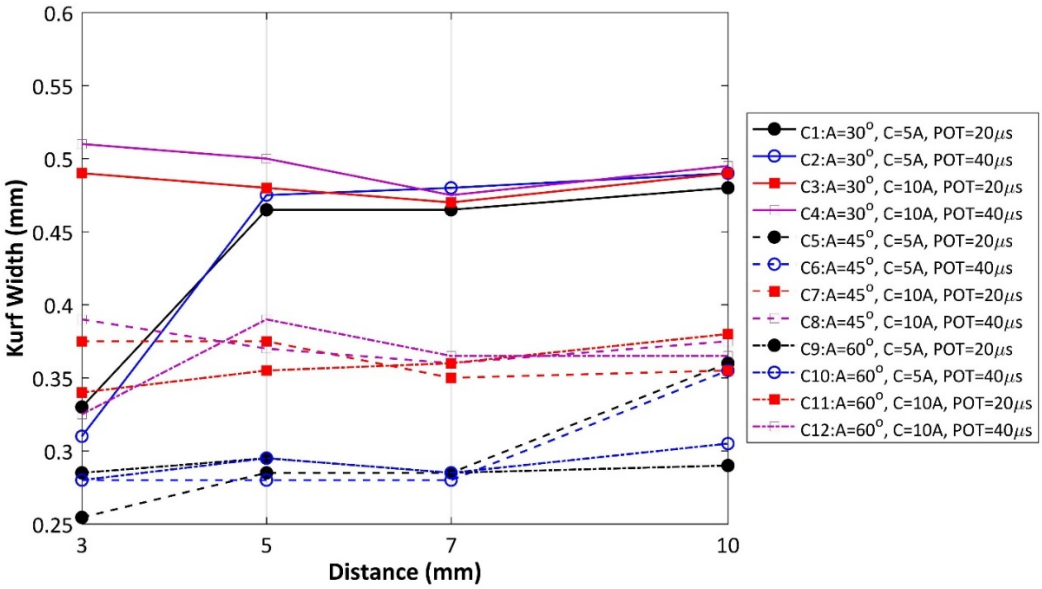

Figure 5 Mean kerf width along the length of the slot

Table 4. Analysis of Variance (ANOVA) for Kerf Width

Source	Degree of Freedom	Adjusted Sum of Squares	Mean Sum of Squares	F-Value	P-Value
Taper Angle (A)	2	0.083816	0.041908	52.94	0.000
Current (C)	1	0.010944	0.010944	13.83	0.003
Pulse-off Time (POT)	1	0.002552	0.002552	3.22	0.098
Taper Angle*Current	2	0.004316	0.002158	2.73	0.106
Taper Angle*Pulse-off Time	2	0.002845	0.001423	1.80	0.208
Current*Pulse-off Time	1	0.002168	0.002168	2.74	0.124
Taper Angle*Current*Pulse-off Time	2	0.005410	0.002705	3.42	0.067
Error	12	0.009499	0.000792		
Total	23				

Figure 6 shows the variation of mean kerf width by varying the process parameters. The figure shows that the mean kerf width decreases with the increase in taper angle due to the higher surface area exposed to the eroding EDM wire. The large surface area exposed to the wire EDM causes the erosion density to be distributed, causing a decrease in kerf width. Figure 6 shows that amassed current increases the kerf width because of the high erosion rate, resulting in a large kerf width. Figure 6 also indicates that the kerf width is amplified with the increase in POT, but as per ANOVA, the F-value is 3.22, which is quite low as comparred to the F-value of taper angle and current. Hence, the effect of POT is insignificant having a P-value < 0.05.

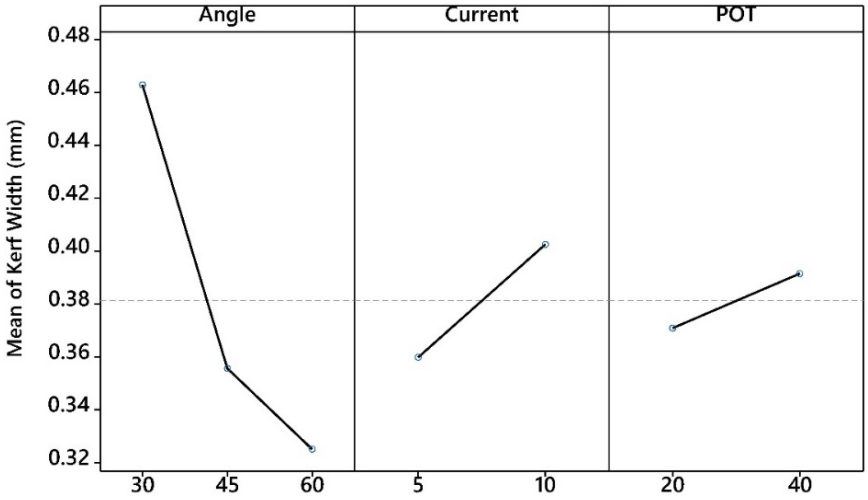

Figure 6 Main effects of mean kerf width

Surface Roughness

Analysis of Variance (ANOVA) for the surface roughness measured on the eroded carbon steel blanks is presented in Table 5. It suggests that none of the parameter and their interaction significantly has P-values higher than 5%. Due to the limited levels of parameters recommended for steel, the significance of process parameters and interactions seem minimal.

Table 5. Analysis of Variance (ANOVA) for surface roughness

Source	Degree of Freedom	Adjusted Sum of Squares	Mean Sum of Squares	F-Value	P-Value
Taper Angle (A)	2	0.0001262	0.0000631	3.06	0.084
Current (C)	1	0.0000012	0.0000012	0.06	0.812
Pulse-off Time (POT)	1	0.0000024	0.0000024	0.12	0.738
Taper Angle*Current	2	0.0000245	0.0000123	0.60	0.567
Taper Angle*Pulse-off Time	2	0.0000323	0.0000161	0.78	0.479
Current*Pulse-off Time	1	0.0000528	0.0000528	2.56	0.135
Taper angle*Current*Pulse-off Time	2	0.0000263	0.0000131	0.64	0.546
Error	12	0.0002472	0.0000206		
Total	23				

Figure 7 shows the varying mean surface roughness with the change in process parameters. Figure 8 also supports the ANOVA presented in Table 5 pertaining to the insignificance of the process parameters and their interactions.

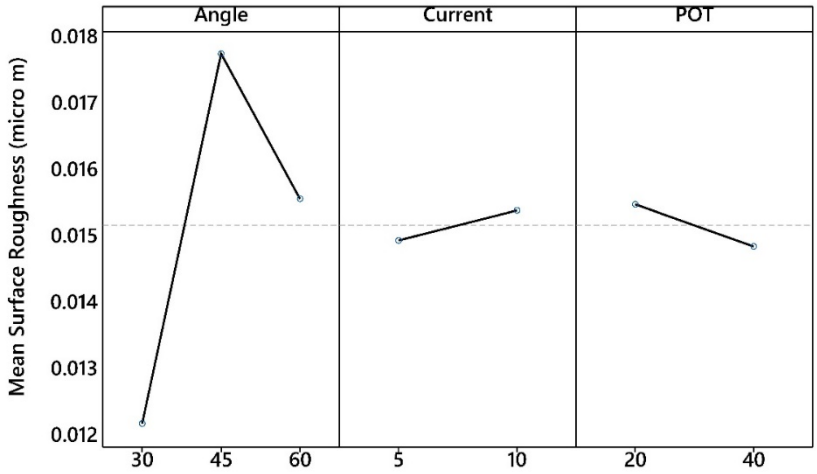

Figure 7 Main effects of mean surface roughness

Material Removal Rate (MRR)

Analysis of Variance (ANOVA) for MRR is presented in Table 6. A P-value less than 5% shows that the current, pulse-off time, taper angle, and taper angle/pulse-off time interact in order of their high F-values and influence and thus, have a significant impact over MRR. It depicts that the alternate hypothesis is valid for these parameters.

Figure 8 shows the trend of MRR with varying WEDM parameters and indicates that with the increase in the taper angle, the material removal rate decreases. This is due to the fact that the surface area exposed to the eroding wire increases with the increase in taper angle. Hence, during the wire EDM process, emitting sparks are distributed over the increased surface area, causing a lower erosion rate. It results in decreased MRR over the large exposed surface area in higher taper angles. Figure 8 also illustrates that MRR enhances with the higher current and reduces with the higher pulse-off time. This is due to the high erosion rate at higher current and lower erosion rate due to the increase in pulse-off time.

Table 6. Analysis of Variance (ANOVA) for Material Removal Rate (MRR)

Source	Degree of Freedom	Adjusted Sum of Squares	Mean Sum of Squares	F-Value	P-Value
Taper Angle (A)	2	61.493	30.747	48.66	0.000
Current (C)	1	88.603	88.603	140.22	0.000
Pulse-off Time (POT)	1	67.445	67.445	106.73	0.000
Taper angle*Current	2	4.565	2.283	3.61	0.059
Taper Angle*Pulse-off Time	2	17.503	8.751	13.85	0.001
Current*Pulse-off Time	1	0.486	0.486	0.77	0.398
Taper angle*Current* Pulse-off Time	2	4.546	2.273	3.60	0.060
Error	12	7.583	0.632		
Total	23				

Figure 9 presents the variation in mean MRR with the interactive influence of controllable parameters. The interaction effect of the taper angle with pulse-off time has the highest effect over MRR. If the taper angle and pulse-off time are increased, MRR drops significantly due to the low erosion rate and increases in the exposed

erosion area. A higher decreasing rate is observed when the pulse-off time is set at 20μs. Other interaction effects show an insignificant change in the MRR, evidenced by the P-values higher than 5% (see Table 6).

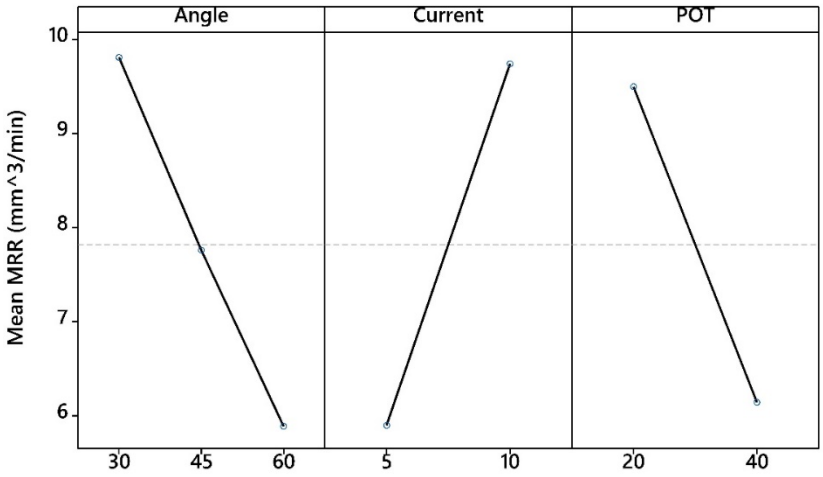

Figure 8 Main effects of mean MRR

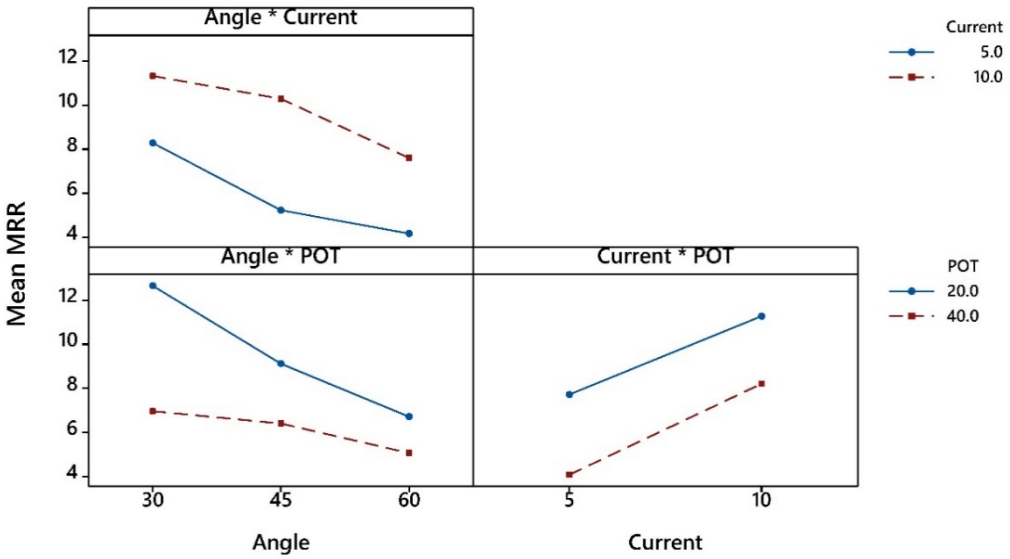

Figure 9 Interaction effects of mean MRR

Wire Wear

Table 7 shows ANOVA for the wire wear during the wire EDM of carbon steel. It shows that taper angle and current are significant over the wire wear, having P-values less than 0.05 and F-values 52.94 and 13.83 respectively.

Table 7. Analysis of Variance (ANOVA) for wire wear

Source	Degree of Freedom	Adjusted Sum of Squares	Mean Sum of Squares	F-Value	P-Value
Taper Angle (A)	2	0.083816	0.041908	52.94	0.000
Current (C)	1	0.010944	0.010944	13.83	0.003
Pulse-off Time (POT)	1	0.002552	0.002552	3.22	0.098
Taper Angle*Current	2	0.004316	0.002158	2.73	0.106
Taper Angle*Pulse-off Time	2	0.002845	0.001423	1.80	0.208
Current*Pulse-off Time	1	0.002168	0.002168	2.74	0.124
Taper Angle*Current*Pulse-off Time	2	0.005410	0.002705	3.42	0.067
Error	12	0.009499	0.000792		
Total	23				

Figure 10 presents the trend in wire wear with respect to controllable process parameters. It shows that increasing the taper angle increases the wire wear, which is due to the higher exposure of wire with the larger surface area during the wire EDM process. A high heat zone is formed around the wire during the WEDM process, whereby a small amount of current does not cause significant erosion. Instead, it disseminates in the form of heat. In the case of 10A current, the wire wear is decreased due to the effective erosion and its effective distribution over the exposed surface of the blank.

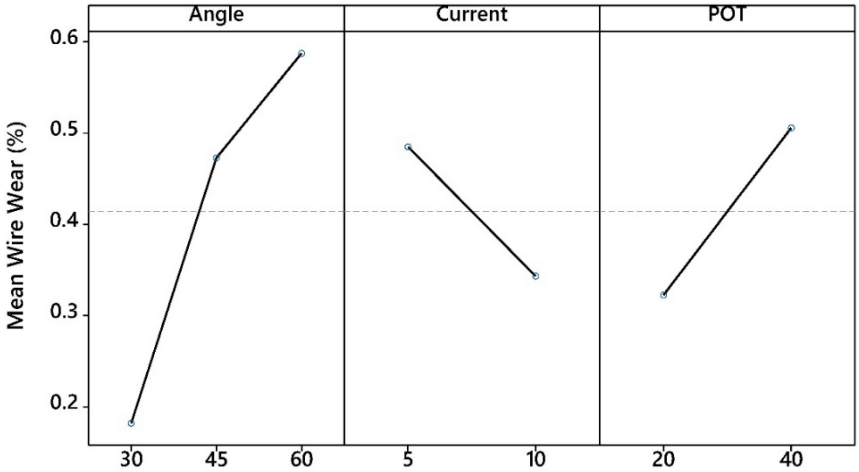

Figure 10 Main effects of mean wire wear

Regression Models for the Response Variables

Regression models have been developed to relate the wire EDM process parameters for the carbon steel 1020 with the response variable. These can be predicted using the regression models for the corresponding values of the controllable parameters. In these regression equations, the effect of controllable parameters is the coefficient of each parameter or interaction, which shows the weightage of these parameters over the response variables. The following equation shows the regression models for the kerf width (KW), surface roughness (SR), MRR and wire wear (WW) respectively.

$$KW = 0.755 - 0.0206A + 0.0145C + 0.0043\mathrm{PO}T + 0.0002A^2 + 0.0001(A \cdot C) - 0.0004(C \cdot POT) \quad (2)$$

$$SR = -0.0211 + 0.0013A + 0.0016C + 0.0001(A \cdot POT) - 0.0001(C \cdot POT) \quad (3)$$

$$MRR = 24.92 - 0.387A + 0.481C - 0.513POT + 0.0004A^2 + 0.0026(A \cdot C) + 0.0067(A \cdot POT) + 0.0057(C \cdot POT) \quad (4)$$

$$WW = -1.491 + 0.0507A + 0.1035C + 0.0066POT + 0.0004A^2 - 0.0017(A \cdot C) + 0.0004(A \cdot POT) - 0.0018(C \cdot POT) \quad (5)$$

Here, A denotes the taper angle, C denotes current, and POT stands for the pulse-off time. Regression models have the effect of main factors, such as A, C and POT, whereas it also shows the effect of interaction of factors over the response variable, such as A·C, A·POT and C·POT. The other interaction of factors having coefficient less than 10^{-5} are not significant and hence eliminated from the regression models. It can be seen from equations that the lower coefficients (10^{-4}) represent lower weightage of parameters over the response variables, which is also clear from ANOVA of the response variables.

Multi-objective Optimization Using NSGA-II

Controllable parameters of the wire EDM used in this research are optimized for the favourable response variables. Genetic algorithm function of MATLAB software has been used to optimize each response variable individually to analyse the effects of process parameters separately. The following equation relates to the functions with the response variables for optimization.

$$f_1(p) = KW(A, C, POT) \quad (6)$$

$$f_2(p) = SR(A, C, POT) \quad (7)$$

$$f_3(p) = MRR(A, C, POT) \quad (8)$$

$$f_4(p) = WW(A, C, POT) \quad (9)$$

Where $\boldsymbol{p}$ denotes the process parameters collectively. The objective functions can be described as

$$\mathrm{z} = \min [f_1(p) \quad f_2(p) \quad -f_3(p) \quad f_4(p)] \quad (11)$$

Here, it is to be noted that MRR is maximized, hence $-\boldsymbol{f_3(p)}$ shows the minimization of the opposite function. The upper and lower bounds of optimization are defined as level 1 and level 2 of the current and pulse off time, as defined in 2. For the taper angles of 30°, 45°, and 60°, the results of individual optimization of each response variable is shown in Table 8.

Table 8. Optimized process parameters for minimization of individual response variable using GA.

Taper Angle (Degree)	Process Parameters		Kerf Width (mm)	Surface Roughness (μs)	MRR (mm^3/min)	Wire Wear (Percentage)
	Current (Ampere)	Pulse off Time (μs)				
30	5	40	0.3795(min)	0.0120	-5.185	0.3165
	10	40	0.3870	0.0092(min)	-9.180	0.2190
	10	20	0.4410	0.0156	-14.220(min)	0.2070
	5	20	0.3935	0.0125	-10.825	0.1245(min)
45	5	40	0.2445(min)	0.0189	-4.045	0.7395
	5	20	0.2885	0.0167(min)	-7.675	0.4275
	10	20	0.3435	0.0202	-11.265(min)	0.3825(min)
60	5	40	0.1995(min)	0.0182	-3.085	0.9825
	5	20	0.2735	0.0133(min)	-4.705	0.5505
	10	20	0.3360	0.0171	-8.490(min)	0.3780(min)

It can be seen from the table that the optimal process parameter providing the minimum value of one response variable does not guarantee the minimum response for the other variable. In a few cases, common minimal values are attained for the optimal parameters such as in the case of 45° taper angle cut with current 10A and pulse-off time of 20μs. A similar situation is observed in the 60° taper blank with parameter 10A 20μs. Hence, optimization of single response variable is not feasible, since it provides unacceptable results for the other response variables. A multi-variable, multi-objective Genetic Algorithm (GA) optimization has been applied using a computer prorgamme written in MATLAB software. NSGA-II algorithm is applied, which is a fast elitist sorting genetic algorithm to determine the optimal solutions for the minimization of objective function z. In the GA algorithm, parameters are set to the population size of 50, cross-over fraction 0.8, mutation fraction 0.4, elite count of population 0.05, and max iteration 200.

The built-in function of Pareto optimal front offers multi-solutions, complying with the objective function z and hence provides a range of solutions. Since there are four different objective functions, which have entirely different trends as evident from Table 8, hence no single solution is possible for such problems, which is also confirmed in the literature (Mathworks, 2020; Simon, 2020). Using Pareto front, 19, 19, and 46, solutions were found based on the precision of up to 10^{-6} for each of the 30°, 45°, and 60° respectively. The results obtained through the hybridization with GA to obtain the local optimization is listed in Table 9. The response variable is not dominant and provides much better trade-off than the outcomes presented in Table 8. It also shows the percent change in the response variable as compared to these measured through the experimental results to the corresponding values. Such as, for the 30° taper angle work piece and the parameters 10A and 20μs, the measured four response variables from Table 4 are 0.4825mm, 0.015μm, 13.45mm^3/min and 0.1581%. Whereas, for the same blank, optimal parameters of 9.9894A and 20.25μs provide the variables 0.4402mm, 0.0154μm, 14.148 mm3/min, and 0.2069%. Hence, it corresponds changes of 9.61%, -3.18%, -4.94%, -23.62% in the response variable. The negative sign shows the decrease in response variable and the positive sign shows the increase. The decrease in response variables is the intended result in the case of kerf width, surface roughness, and wire wear due to minimization, whereas increases are favourable for the MRR due to intended maximization.

It can be seen from the above table that the best results are achieved for the 30° taper angle work piece, where the kerf width is higher, whereas the least surface finish and wire wear are achieved with the best possible MRR. Table 9 shows the minimum kerf width, surface roughness, and wire wear and the maximum MRR. The most feasible values of current are near 10A for all the work pieces with any of the three taper angles. Whereas, pulse-off time around 20ms seems to be suitable for all three taper angle work pieces as evidenced by the optimization results.

Table 9. Multi-objectively optimized process parameters using the Genetic Algorithm.

Taper Angle (Degree)	Process Parameters		Kerf Width (mm)	Surface Roughness (μs)	MRR (mm^3/min)	Wire Wear (Percentage)
	Current (Ampere)	Pulse off Time (μs)				
30	9.9894	20.25	0.4402 (9.61%)	0.0154 (-3.18%)	14.148 (-4.94%)	0.2069 (-23.62%)
45	9.9987	20.01	0.3434 (5.92%)	0.0201 (-4.23%)	11.263 (6.82%)	0.3825 (-6.65%)
60	10.000	20.04615	0.3357 (6.87%)	0.0170 (2.48%)	8.4874 (-1.03%)	0.3786 (-0.18%)

Table 9 clearly shows that the higher value of current (10A) and lower value of pulse-off time (20μs) are recommended by the optimization results. It is contrary to the optimization results presented for the titanium, aluminium, and higher grades of the steel, where sometimes lower currents and higher pulse-off time are important to cool down the cutting interface. Else, it results in a higher surface roughness and kerf width, causing the higher melt rate of the metal (Liao et al. (2004) Kumar and Singh, 2018, Wasif et al., 2020).

CONCLUSION

Investigation of wire EDM process effects over the kerf width, surface roughness, MRR, and wire wear have been studied over the tapered blank of carbon steel 1020. Based on the results and subsequent analysis, the following conclusions can be drawn.

- Taper angle and current have substantial effects over the kerf width of slots generated in carbon steel 1020 taper blanks. Kerf width along the slot length usually remains the same, whereas a smaller increase is observed when the higher taper angle blanks are cut through the wire EDM.

- The relation between the kerf width and the taper angle is inverse in carbon steel 1020. Increasing the taper angle decreases the kerf width. It also increases with increasing the current, whereas it decreases with the increased pulse-off time.

- No considerable influence of any process parameter is seen over the surface finish of the tapered blank. It may be due to the levels of the factors selected in this research, which are based on the recommended parameters' level for the steels.

- All three controllable process parameters, along with the interaction of the current with pulse-off time, drastically impact MRR. It decreases with the simultaneous increase in taper angle and pulse-off time, due to more substantial area of exposure and distribution of erosion over the larger area.

- During the wire EDM of carbon steel 1020, it is revealed that the taper angle and current influence the wire wear. A high wire wear is observed in the blank with the increase in taper angle and current, whereas the taper angle significantly influences the wire wear as compared to the current.

- The relationship between the controllable parameters of wire EDM and the response variables is developed and presented in this research, which can predict the wire EDM outcomes.

- The multi-objective optimization using genetic algorithm is applied to the regression models to attain the optimized current and pulse-off time values for three different tapered blanks. Optimal results suggest that the higher current (10A) and lower pulse off time (20μs) provide favourable conditions for all the four response variables, unlike the titanium and high grade steels.

The data and analysis presented in this research can be applied in the industry and the regression models can be used to forecast the kerf width, surface roughness, MRR, and wire wear for the desirable sets of conditions. These parameters can be used to cut the geometries of the complicated die tool, punches, and other intrinsic parts used in the aircraft and other machine tool components. The optimal value of process parameters can be applied during the production process for the carbon steel 1020 to achieve economy and productivity.

ACKNOWLEDGEMENTS

We present our immense regards to Mr. Muhammad Ali (Technician) of Advanced Manufacturing Laboratory at NED University of Engineering and Technology for providing assistance during the research study experiments.

REFERENCES

Abinesh, P., Varatharajan, K., Kumar, G.S. 2014. Optimization of Process Parameters Influencing MRR, Surface Roughness and Electrode Wear During Machining of Titanium Alloys by WEDM, Int. J. Eng. Res. Gen. Sci. 2(4): 719-729.

Alduroobi, A.A.A., Ubaid, A.M., Tawfiq, M.A. et al. 2020. Wire EDM process optimization for machining AISI 1045 steel by use of Taguchi method, artificial neural network and analysis of variances. Int. J. Syst. Assur. Eng. Manag. 11: 1314–1338. DOI: https://doi.org/10.1007/s13198-020-00990-z

Asgar, M.E. and Singholi, A.K.S. 2018. Parameter study and optimization of WEDM process: A Review, IOP Conf. Series: Materials Science and Engineering 404, Lucknow, India.

Arunadevi Y. L, M., Prakash, C. P. S. 2021. Predicton of MRR & Surface Roughness in Wire EDM Machining using Decision Tree and Naive Bayes Algorithm, International Conference on Emerging Smart Computing and Informatics (ESCI), 2021, pp. 527-532, DOI: 10.1109/ESCI50559.2021.9396857.

Babu, T.V., Soni, J.S. 2017. Optimization of process parameters for surface roughness of Inconel625 in Wire EDM by using Taguchi and ANOVA method, Int. J. Curr. Eng. Technol. 7(3): 1127-1131.

Conde, A., Sanchez, J.A., Plaza, S., Ostolaza, M., Puerta, de la, Li, Z. 2018. Experimental Measurement of Wire-lag Effect and Its Relation with Signal Classification on Wire EDM, In Proceeding of the CIRP 68, Bilbao, Spain: 132-137. DOI: https://doi.org/10.1016/j.procir.2017.12.035

Dayakar, K., Krishnam Raju, K.V. M, Raju, C.R.B. 2019. Prediction and optimization of surface roughness and MRR in wire EDM of maraging steel 350, Materials Today 18(6): 2123-2131. DOI: https://doi.org/10.1016/j.matpr.2019.06.635

Dewangan, S., Mainwal, N., Khandelwal, M., Jadhav, P.S. 2019. Performance analysis of heat treated AISI 1020 steel samples on the basis of various destructive mechanical testing and microstructural behaviour, Aust. J. Mech. Eng. online: 2204-2253. DOI: 10.1080/14484846.2019.1664212.

El-Hofy, H. A. 2005. Advanced Machining Processes: Nontraditional and Hybrid Machining Processes, McGraw-Hill, USA.

El-Bahloul, S.A. 2020. Optimization of wire electrical discharge machining using statistical methods coupled with artificial intelligence techniques and soft computing. SN Appl. Sci. 2: 49. DOI: https://doi.org/10.1007/s42452-019-1849-6

Gauri, S.K. and Chakraborty, S. 2009. Optimisation of multiple responses for WEDM processes using weighted principal components, Int. J. Adv. Manu. Tech. 40: 1102–1110. DOI: 10.1007/s00170-008-1429-1

Huang, J.T., Liao, Y.S. 2003. Optimization of machining parameters of Wire-EDM based on Grey relational and statistical analyses, Int. J. Prod. Res. 41(8): 1707-1720. https://doi.org/10.1080/1352816031000074973

Jameson, E. 2001. Electrical Discharge Machining, Society of Manufacturing Engineers (SME). USA.

Kamei, T., Okada, A., Okamoto, Y. 2016. High-speed Observation of Thin Wire Movement in Fine Wire EDM, In Proceeding of the 18th CIRP Conference on Electro Physical and Chemical Machining (ISEM XVIII), Tokyo, Japan, April 2016: 596-600.

Kanlayasiri, K., Boonmung, S. 2007. Effects of wire-EDM machining variables on surf ace roughness of newly developed DC 53 die steel: Design of experiments and regression model, J. Mater. Process. Technol. 192: 459-464.

Klocke, F., Welling, D., Klink, A., Veselovac, D., Nöthe, T., Perez, R. 2014. Evaluation of Advanced Wire-EDM Capabilities for the Manufacture of Fir Tree Slots in Inconel 718, In Proceeding of the 6th CIRP International Conference on High Performance Cutting (HPC 2014), Berkeley, USA, June 2014: 430-435. DOI: https://doi.org/10.1016/j.procir.2014.03.039

Kumar, R. and Singh, I. 2018. Productivity improvement of micro EDM process by improvised tool, Precis. Eng. 51: 529-535.

Liao, Y.S., Yu, Y.P. 2014. Study of specific discharge energy in WEDM and its application, Int. J. Mach. Tools Manuf. 44(12): 1373-1380. https://doi.org/10.1016/j.ijmachtools.2004.04.008

Majumder, H. and Maity, K. 2017. Multi-Response Optimization of WEDM Process Parameters Using Taguchi Based Desirability Function Analysis, IOP Conf. Series: Material Science Engineering 338, Rourkela, India.

Matheworks. 2020. Global Optimization Toolbox, MATLAB User's Guide, Mathworks Inc, USA.

Priyadarshini, M., Biswas, C.K., Behera, A. 2019. Machining of sub-cooled low carbon tool steel by wire-EDM, Mater. Manuf. Process. 34(12): 1316-1325. DOI: https://doi.org/10.1080/10426914.2019.1662035

Priyadarshini, M., Biswas, C.K., Behera, A. 2019. Grey-Taguchi optimization of Wire-EDM parameters for P20 tool steel, In Proceeding of the 5th International Conference on Mechatronics and Robotics Engineering, ICMRE '19, Rome, Italy, February 2019: 5-8. DOI: https://doi.org/10.1145/3314493.3314506

Rao, P.S., Ramji, K., Satyanarayana, B. 2016. Effect of wire EDM conditions on generation of residual stresses in machining of aluminum 2014 T6 alloy, Alex. Eng. J. 55(2): 1077-1084. DOI: 10.1016/j.aej.2016.03.014

Rajmohan, K., Kumar, A.S. 2017. Experimental investigation and prediction of optimum process parameters of micro-wire-cut EDM of 2205 DSS, Int. J. Adv. Manuf. Tech. 93: 187-201. https://doi.org/ 10.1007/s00170-016-8615-3

Raksiri, C., Chatchaikulsiri, P. 2010. CNC Wire-Cut Parameter Optimized Determination of the Stair Shape Work piece, Int. J. Mech. Mechatron. Eng. 4(10): 924-929.

Reddy, V.C., Deepthi, N., Jayakrishna, N. 2015. Multiple Response Optimization of Wire EDM on Aluminium HE30 by using Grey Relational Analysis' In Proceeding of the Materials Today 2(4–5), Hyderabad, India, February 2015: 2548-2554.

DOI: https://doi.org/10.1016/j.matpr.2015.07.201

Sahoo, S.K., Naik, S.S., Rana, J. 2019. Experimental Analysis of Wire EDM Process Parameters for Micromachining of High Carbon High Chromium Steel by Using MOORA Technique, Micro and Nano Machining of Engineering Materials. Materials Forming, Machining and Tribology. Springer, Cham. DOI: 10.1007/978-3-319-99900-5_7

Shadab, M., Singh, R., Rai, R.N. 2019. Multi-objective Optimization of Wire Electrical Discharge Machining Process Parameters for Al5083/7% B4C Composite Using Metaheuristic Techniques, Arab. J. Sci. Eng. 44: 591. DOI: https://doi.org/10.1007/s13369-018-3491-9

Shihab, S.K. 2018. Optimization of WEDM Process Parameters for Machining of Friction-Stir-Welded 5754 Aluminum Alloy Using Box–Behnken Design of RSM, Arab. J. Sci. Eng. 43: 5017-5027. DOI: https://doi.org/10.1007/s13369-018-3238-7

Simon, V. 2019. Multi-objective optimization of hypoid gears to improve operating characteristicsharacteristics', Mech. Mach. Theory. 146: 103727. DOI: 10.1016/j.mechmachtheory.2019.103727

Sommer, C. and Sommer, S. 2017. Complete EDM Handbook, 2nd ed., Advance Pub. Houstan, USA.

Świercz, R., Oniszczuk-Świercz, D., Zawora, J., Marczak, M. 2019. Investigation of the Influence of Process Parameters on Shape Deviation after Wire Electrical Discharge Machining, Arch. Metall. Mater. 64(4): 1457-1462. DOI: 10.24425/amm.2019.130113

Takayama, Y., Makino, Y., Niu, Y., Uchida, H. 2016. The Latest Technology of Wire-cut EDM, In Proceeding of the CIRP 42: 623-626. DOI: 10.1016/j.procir.2016.02.259

Wasif, M., Iqbal, S.A., Fatima, A., Yaqoob, S., Tufail, M. 2020. Experimental investigation for the effects of wire EDM process parameters over the tapered cross-sectional work pieces of titanium alloys (Ti6Al-4V). Mech. Sci. 11: 221–232. DOI: https://doi.org/10.5194/ms-11-221-2020

Welling, D. 2014. Results of Surface Integrity and Fatigue Study of Wire-EDM Compared to Broaching and Grinding for Demanding Jet Engine Components Made of Inconel 718, In Proceeding of the 2nd CIRP Conference on Surface Integrity (CSI), Nottingham, UK, May 2014: 339-344. https://doi.org/10.1016/j.procir.2014.04.057